Evidence for Long Localization Length along b Axis $PrBa_2Cu_3O_7$ in a Axis $YBa_2Cu_3O_7/a,b$ Axis $PrBa_2Cu_3O_7$ Superlattices

Y. Suzuki, J.-M. Triscone,* C. B. Eom,† M. R. Beasley, and T. H. Geballe
Department of Applied Physics, Stanford University, Stanford, California 94305-4090
(Received 29 December 1993)

We have investigated resistive transitions of a axis $YBa_2Cu_3O_7/a,b$ axis $PrBa_2Cu_3O_7$ superlattices in a magnetic field to study the correlation length of vortices along the a axis direction of $YBa_2Cu_3O_7$ across an a,b axis oriented $PrBa_2Cu_3O_7$ barrier. The correlation of vortices across up to 480 Å of $PrBa_2Cu_3O_7$ is evidence consistent with long proximity coupling coherence lengths in $PrBa_2Cu_3O_7$ found in sandwich type $YBa_2Cu_3O_7/PrBa_2Cu_3O_7/YBa_2Cu_3O_7$ Josephson junctions. Investigation of a-b plane and b axis transport of undoped and cobalt doped $PrBa_2Cu_3O_7$ films suggests that a long localization length along the b axis of $PrBa_2Cu_3O_7$ is the origin of this long range proximity coupling.

PACS numbers: 74.80.Dm, 74.72.Jt

The absence of superconductivity and the insulating-semiconducting behavior in $PrBa_2Cu_3O_7$ (PBCO) at low temperature are still not well understood. In particular a long proximity coupling coherence length of PBCO [sandwiched between two $YBa_2Cu_3O_7$ (YBCO) layers] along the a-b plane is at odds with Mott variable range hopping (VRH) behavior seen in *some* PBCO films. VRH behavior is dominated by phonon assisted hopping of carriers between localized states close in energy to one another. Since inelastic scattering mechanisms such as VRH are intrinsically pair breaking, they cannot account for the long proximity coupling coherence length of PBCO in the a-b planes. Many groups have fabricated a axis YBCO/PBCO/YBCO trilayers and not all have found unusually long proximity coupling coherence lengths. On the one hand, Barner *et al.* show critical currents across up to 1500 Å of PBCO [1]. Hashimoto *et al.* show a Farunhofer diffraction pattern of I_c versus field in their junctions with a PBCO barrier of 1000 Å [2]. On the other hand, Lew *et al.* deduce the coherence length of PBCO to be 30 Å [3]. The results of these groups are not necessarily in disagreement, however, because in none of these investigations has the oxygen content of PBCO been controlled. Although oxygen deficient PBCO may exhibit VRH, optimally oxygen doped PBCO shows more conductive behavior [4]. A possible explanation perhaps is that bound localized pairs already exist in PBCO, leading to the unusual proximity coupling in PBCO [5].

Based on recent results on the charge distribution of PBCO, Fehrenbacher and Rice have proposed that the CuO chains in PBCO are actually disordered conductors [6,7]. Highly conductive CuO chains in PBCO would provide a natural explanation for the long-range coupling. Indeed, Umezawa *et al.* put forth conductive CuO chains as a possible explanation for the long-range coupling observed in YBCO/PYBCO/YBCO Josephson junctions [8]. Recent studies of a-b plane transport in PBCO by Kabasawa *et al.* suggest that at higher temperatures the a-b planes exhibit VRH whereas at low temperatures and short length scales another more metalliclike mechanism is responsible for a-b plane transport [9]. Very recently Hoffmann *et al.* have probed the CuO chains of PBCO using angular correlation of positron annihilation radiation, revealing locally metallic CuO chains [10]. Although the chains are insulating on a macroscopic scale, they appear locally metallic, giving rise to a long localization length for the carriers. Highly conductive chains would be an appealing explanation of the observed anomalies in the transport in PBCO.

Previous investigation of the resistive transitions of a axis YBCO/PBCO superlattices in a magnetic field has provided additional evidence of long-range coupling across PBCO [11]. In this study, we confirm that conjecture by studying the vortex coupling in adjacent a axis YBCO layers separated by varying thicknesses of a,b axis PBCO from 48 to 480 Å; vortex coupling is measured by activation energies deduced from the thermally activated tails of resistive transitions of YBCO/PBCO superlattices in a magnetic field. The existence of long-range coupling across a,b axis PBCO suggests a long vortex correlation length, a measure of the strength of coupling along a vortex. We proceed to investigate the microscopic origin of such coupling by means of transport studies in oriented PBCO films. By isolating the b axis resistivity in in-plane aligned a axis PBCO films, we find the conductivity along the b axis (CuO chains in parallel with CuO planes) to be higher than that just along the CuO planes which display VRH. This finding along with the long vortex correlation lengths in YBCO/PBCO superlattices provides strong support for assuming that the CuO chains are responsible for the long localization length in PBCO.

The superlattices of a axis YBCO/PBCO have been fabricated by 90° off-axis sputtering in 60 mTorr of Ar and 40 mTorr of O_2 at 640 °C. They all have nominal thicknesses of 2500 Å. These structures exhibit good Rutherford backscattering channeling with $\chi_{min} \sim 3\%$, sharp rocking curves, and sharp satellite peaks from x-ray diffraction analysis (XRD). These YBCO/PBCO superlattices have highly continuous layers and sharp interfaces as seen by cross sectional transmission electron mi-

0031-9007/94/73(2)/328(4)$06.00

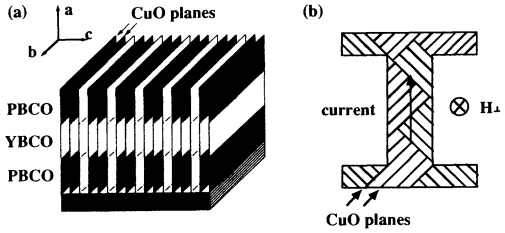

FIG. 1. (a) A schematic of a grain of an a axis YBCO/PBCO superlattice. (b) Current and field configurations of the superlattices.

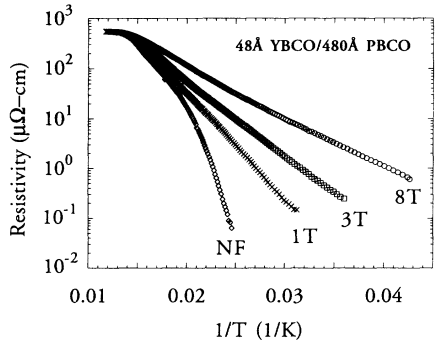

FIG. 2. Resistivity versus inverse temperature for a 48 Å YBCO/480 Å PBCO superlattice in no field and 1, 3, and 8 T. The activation energies are deduced from the tails of the transitions in the interval $10^{-2}\rho_n < \rho < 10^{-4}\rho_n$, where ρ_n is the normal state resistance.

croscopy (TEM) [11,12]. Careful XRD analysis reveals that although the YBCO layers grow with the a axis normal to the substrate, the PBCO layers have a combination of a and b axis growth. In PBCO films the a and b axes are much closer in value than in YBCO so that epitaxial growth of both a and b axis PBCO on a axis YBCO is reasonable. In a or b axis films, the CuO plane is oriented perpendicular to the surface of the substrate and 90° grain boundaries connect adjacent grains. In our YBCO/PBCO superlattices, each CuO plane is made of alternating superconducting and insulating strips as illustrated in Fig. 1(a). The films are patterned such that the CuO planes are at 45° to the direction of macroscopic current flow and the voltage drop is measured along the current flow as shown in Fig. 1(b). Contacts are made by evaporating gold over the edge of the current and voltage pads, thus ensuring uniform current conduction along all YBCO layers. The resistivities of the YBCO layers in the different superlattices scale with layer thickness consistent with uniform conduction through all of the YBCO layers. We have fabricated superlattices with 48 Å YBCO and 48, 192, and 480 Å PBCO; hence even the thinnest layer (48 Å) contains twelve unit cells.

We measure resistive transitions in a field applied perpendicular to the substrate. The field is parallel to all the CuO planes and individual vortex segments are limited in length by the artificial layering. The vortices in the YBCO layers feel a Lorentz force perpendicular to the CuO planes. Vortices in adjacent YBCO layers are coupled to one another when the PBCO layers are thin compared to the proximity coherence length. The resistive transitions in magnetic field exhibit thermally activated behavior. The energies associated with this activated behavior should be sensitive to the coupling between vortices in adjacent YBCO layers. From the tails of these transitions, we have determined the activation energies from plots of $\ln\rho$ vs $1/T$ in the interval $10^{-2}\rho_n < \rho < 10^{-4}\rho_n$, where ρ_n is the normal state resistance. Assuming $U(B,T) = U_0(B)(1 - T/T_c)$ for the temperature dependence of the activation energy, we can express the resistivity ρ as $\rho(T) = \bar{\rho}_0 \exp[-U_0(B)/k_B T]$, where $\bar{\rho}_0 = \rho_0 \exp[U_0(B)/k_B T_c]$. Then we can deduce the extrapolated zero temperature activation energy $U(T=0,B) = U_0(B)$ from the slope of plots of $\ln\rho$ vs $1/T$ (Fig. 2). A plot of $\ln\bar{\rho}_0$ vs $U_{\text{meas}}/k_B T_c$ for all samples and fields is linear with a slope ~ 1, justifying the assumption of a $(1 - T/T_c)$ temperature dependence for $U(B,T)$. In addition, the fits of $\rho(T)$ for the activation energies are accurate to within 7% as the interval of the fit is varied by an order of magnitude.

Figure 3(a) shows that as the PBCO thickness is increased and thus the anisotropy increased, the zero temperature activation energy normalized by $k_B T_c$ decreases. This decrease indicates that neighboring 48 Å a axis YBCO layers are coupled for PBCO thicknesses at least up to 480 Å. Further experiment shows that for larger PBCO thicknesses the adjacent YBCO layers are actually decoupled. Keeping the PBCO thickness at 480 Å, we change the YBCO layer thickness from 48 to 96 Å. As seen from Fig. 3(b), the activation energy is proportional to the thickness of the YBCO layer, as expected when the vortices in adjacent YBCO layers are negligibly coupled.

It is unlikely that epitaxial growth of these superlattices results in shortening of the superconducting layers. In fact cross sectional TEM shows well defined and continuous layers. Furthermore the decrease in activation energies with increasing PBCO layers cannot be explained in terms of interlayer shorts in the smaller period superlattices. For if there were a few interlayer shorts, it would not be energetically favorable for the vortices to thread through superconducting interlayer shorts; instead they would be pinned in the insulating PBCO layers. Therefore the measured vortex transport properties would not show the effect of interlayer shorts, in contrast to experiments which measure vertical transport down through the layers. Only if the density of shorts is large on the coherence length scale would one expect to see the effect of shorts on the measured transport properties of the vortices; cross sectional TEM does not reveal such a high density of shorts. Moreover, the YBCO layer thickness variations of ± 4 Å (i.e., one unit cell), as seen by cross sectional TEM, cannot explain the activation energy differences among the superlattices.

The observed activation energies exhibit a logarithmic

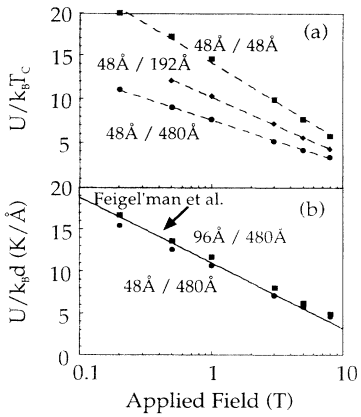

FIG. 3. (a) The activation energies of 48 Å YBCO/48 Å PBCO, 48 Å YBCO/192 Å PBCO, and 48 Å YBCO/480 Å PBCO in magnetic field perpendicular to the YBCO/PBCO layering. (b) The activation energies of the 48 Å YBCO/480 Å PBCO and 96 Å YBCO/480 Å PBCO scale with the YBCO thickness suggesting that vortices in adjacent YBCO layers are negligibly coupled; the logarithmic dependence of activation energies on magnetic field is fit to the prediction by Feigel'man *et al.*

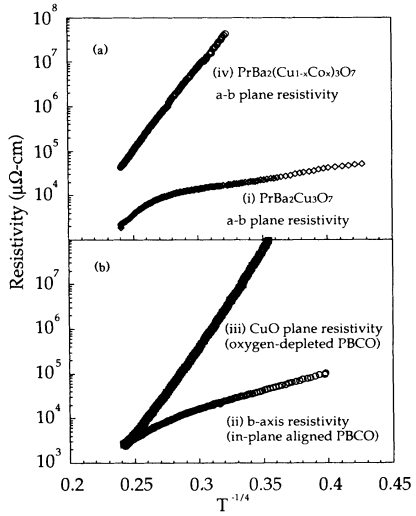

FIG. 4. Resistivity versus $T^{-1/4}$: (a) *a-b* plane resistivity in a *c* axis PBCO film does not exhibit VRH (curve *i*) while *a-b* plane resistivity in a *c* axis Co doped PBCO film does (curve *iv*); (b) *b* axis resistivity of an in-plane aligned *a* axis PBCO film (curve *ii*); a VRH contribution from the CuO planes, obtained from removing oxygen from the CuO chains of an as-grown *c* axis PBCO film (curve *iii*).

dependence on magnetic field. In a later publication we will show that this is in excellent agreement with the theory of Feigel'man, Geshkenbein, and Larkin, which predicts a logarithmic dependence from the plastic deformation of the vortex lattice induced by free dislocation pair formation in the presence of strong pinning [Fig. 3(b)] [13].

The above transport measurements in a magnetic field of YBCO/PBCO superlattices confirm long-range coupling of *a* axis YBCO across *a* and *b* axis PBCO as found in trilayer YBCO/PBCO/YBCO junctions. However, the activation energies are orders of magnitude too large to be explained by magnetic coupling of vortices in the YBCO layers across *insulating* PBCO when the magnetic coupling energies are calculated as the increase in energy due to the interaction of a vortex lattice with a secondary vortex lattice separated by insulating material [14]. Some more coherent elastic conduction mechanism leading to a long localization length for carriers must be present. Highly conductive CuO chains or chain segments in PBCO are an attractive possibility.

Recent results on optical reflectivity of untwinned PBCO indicate that the hole concentration along the chains is unaffected by substitution of Y by Pr whereas the CuO planes of PBCO show an optical response similar to that of $YBa_2Cu_3O_6$ [6]. Those results suggest that in PBCO the CuO planes are insulating while the CuO chains are conducting. In line with those results, Fehrenbacher and Rice propose the electronic structure of PBCO to consist of CuO chains described by a 1D *t-J* model, a mixed valence PrIII-PrIV configuration, and insulating CuO planes [7]. More recently, by studying the angular correlation of positron annihilation radiation in two dimensions, Hoffmann *et al.* have observed a Fermi surface sheet due to the CuO chains in PBCO similar to that in superconducting YBCO, $DyBa_2Cu_3O_7$, and $HoBa_2Cu_3O_7$ [10]. They conclude that although the CuO chains in PBCO remain metallic locally, the macroscopic insulating behavior is a manifestation of the sensitivity of 1D CuO chains in PBCO to disorder.

To determine more directly if the CuO chains are responsible for the observation of a long proximity coherence length in Josephson junctions and the long vortex correlation lengths in superlattices, we studied *c* axis and in-plane aligned *a* axis PBCO films where the *b* axis resistivity has been successfully isolated. Resistivities are plotted as $\ln\rho$ vs $T^{-1/4}$ so that linearity is indicative of VRH behavior where transport occurs via inelastic hopping between localized states [15]. In the case of conventional *c* axis films, transport occurs via the planes and chains. Curve *i* in Fig. 4 is representative of *c* axis PBCO films which exhibit VRH at higher temperatures with a flattening out at low temperatures. Because of the twinning in *c* axis films, on average the current flows half of the time along the *a* axis (just along the CuO planes) and half of the time along the *b* axis (along both the CuO planes and CuO chains); therefore the measured resistivity is a combination of CuO planes and CuO chains.

To investigate whether the flattening out at low temperatures can be attributed to the CuO chains, we then studied in-plane aligned *a* axis PBCO films on (100)$LaSrGaO_4$; they were grown using the same techniques as in-plane aligned *a* axis YBCO films [16]. In these PBCO films where we have isolated the *b* axis direction, we observe a temperature dependence of *b* axis resistivity roughly similar to that of the *a-b* plane in *c*

axis films, i.e., a flattening out of the resistivity at low temperatures (curve *ii* in Fig. 4). Noting that the chain contribution can be removed by oxygen depletion, we can isolate the plane contribution. After we anneal *c* axis and in-plane aligned *a* axis PBCO films in an oxygen poor atmosphere of 3 Torr at 550 °C for 1 h, the films exhibit VRH behavior (curve *iii* in Fig. 4). Successive anneals in 3 Torr, 3 mTorr, and 0.4 mTorr of O_2 at 550 °C, corresponding to oxygen content estimates of 6.5, 6.2, and 6.0, respectively, were performed on the *c* axis PBCO films. They maintained VRH temperature dependences. The oxygen contents were estimated by measuring the *c* axis lattice parameter and the resistivity of *c* axis YBCO films annealed along with the PBCO films. These anneals reveal the sensitivity of the temperature dependence of PBCO to oxygen content. The VRH behavior observed after depletion of oxygen from the CuO chains suggests that the CuO planes in PBCO are VRH. Therefore the flattening out of the resistivity at low temperatures in as-grown PBCO films (curves *i* and *ii*) suggests that the highly conductive CuO chains dominate transport.

To substantiate the hypothesis that the CuO planes of as-grown PBCO exhibit VRH and the CuO chains do not, we have investigated $PrBa_2Cu_3O_7$ doped with 5% cobalt on the copper site [curve *iv* in Fig. 4(a)]. Studies of $YBa_2(Cu_{1-x}Co_x)_3O_7$ (YBCCO) show that the cobalt substitutes for copper on the chain sites and only distorts the chains leaving the CuO planes intact [17]. Similarities in transport properties of YBCCO and $YBa_2Cu_3O_{7-\delta}$ suggest that cobalt doping is chemically equivalent to oxygen depletion [18]. Now in $PrBa_2(Cu_{1-x}Co_x)_3O_7$ (PBCCO) the transport in the CuO planes cannot be completely unaffected by the cobalt doping. However, by analogy to cobalt's effects in YBCO, there should be little charge transfer to the planes in PBCO. Therefore, *a-b* plane transport of *c* axis PBCCO with $x=0.05$ should be an indication of CuO plane transport of PBCO. In fact, *a-b* plane transport of PBCCO does show VRH (curve *iv*). Removal of oxygen from the PBCCO films by annealing in an oxygen poor atmosphere at 550 °C does not change the VRH behavior, thus confirming our model that in PBCO, the CuO planes exhibit VRH whereas the CuO chains have a much higher conductivity and a non-VRH temperature dependence. This is consistent with the model presented by Fehrenbacher and Rice [7].

In conclusion, in *a* axis YBCO/PBCO superlattices we observe coupling of vortices across *a,b* axis PBCO of up to 480 Å. This is consistent with the long proximity coupling coherence lengths seen in YBCO/PBCO/YBCO sandwich type Josephson junctions. Our study of *a-b* plane and *b* axis transport of undoped and cobalt doped $PrBa_2Cu_3O_7$ films reveals VRH CuO planes and a long localization length along the CuO chains in $PrBa_2Cu_3O_7$, consistent with our vortex coupling experiments and recent theoretical work based on the electronic structure of $PrBa_2Cu_3O_7$.

We thank L. L. H. King and A. W. Sleight for providing us with the Co doped PBCO target, Komatsu Co. Ltd. for providing us with $LaSrGaO_4$ substrates, and S. Doniach, D. Lew, and W. R. White for helpful discussions. We acknowledge the Air Force Office of Scientific Research and the Electrical Power Research Institute for their support. Y.S. acknowledges partial financial support from the National Science Foundation.

*Presently at DPMC Université de Genève 24 Quai E. Ansermet, 1211 Genève 4, Switzerland.

†Presently at Department of Mechanical Engineering and Materials Science, Duke University, Durham, NC 27708-0300.

[1] J. B. Barner, C. T. Rogers, A. Inam, R. Ramesh, and S. Bersey, Appl. Phys. Lett. **59**, 742 (1991).

[2] T. Hashimoto, M. Sagoi, Y. Mizutani, J. Yoshida, and K. Mizushima, Appl. Phys. Lett. **60**, 1756 (1992).

[3] D. Lew, Y. Suzuki, C. B. Eom, Mark Lee, J.-M. Triscone, and T. H. Geballe, M. R. Beasley, Physica (Amsterdam) **185–189C**, 2553 (1991).

[4] B. Fisher, J. Genossar, L. Patlagan, and J. Ashkenazi, Phys. Rev. B **43**, 2821 (1991); M. E. López-Morales, D. Ríos-Jara, J. Tagüeña, R. Escuedero, S. LaPlaca, A. Bezinge, V. Y. Lee, E. M. Engler, and P. M. Grant, Phys. Rev. B **41**, 6655 (1990).

[5] S. Doniach and M. Inui, Phys. Rev. B **41**, 6668 (1990).

[6] K. Takenaka, Y. Imanaka, K. Tamasaku, T. Ito, and S. Uchida, Phys. Rev. B **46**, 5833 (1992).

[7] R. Fehrenbacher and T. M. Rice, Phys. Rev. Lett. **70**, 3471 (1993); J. J. Neumeier, M. B. Maple, and M. S. Torikachvili, Physica (Amsterdam) **156C**, 574 (1988).

[8] T. Umezawa, D. Lew, S. K. Streiffer, and M. R. Beasley, Appl. Phys. Lett. **63**, 3321 (1993).

[9] U. Kabasawa, Y. Tarutani, M. Okamoto, T. Fukuzawa, A. Tsukamoto, M. Hiratani, and K. Takagi, Phys. Rev. Lett. **70**, 1700 (1993).

[10] L. Hoffmann, A. A. Manuel, M. Peter, E. Walker, M. Gauthier, A. Shukla, B. Barbiellini, S. Massidda, Gh. Adam, S. Adam, W. N. Hardy, and Ruixing Liang, Phys. Rev. Lett. **71**, 4047 (1993).

[11] J.-M. Triscone, C. B. Eom, Y. Suzuki, and T. H. Geballe, J. Alloys Compounds **183**, 224 (1992).

[12] C. B. Eom, A. F. Marshall, J.-M. Triscone, B. Wilkens, S. S. Laderman, and T. H. Geballe, Science **251**, 780 (1991).

[13] M. V. Feigel'man, V. B. Geshkenbein, and A. I. Larkin, Physica (Amsterdam) **167C**, 177 (1990); J. J. Neumeier, M. B. Maple, and M. S. Torikachvili, Physica (Amsterdam) **156C**, 574 (1992).

[14] J. R. Clem, Phys. Rev. B **9**, 898 (1974).

[15] Experimentally the oxygen depleted PBCO resistivities fit to $\rho_0\exp(T_0/T)^{1/4}$ (3D VRH) just as well as to $\rho_0\exp(T_0/T)^{1/3}$ (2D VRH).

[16] Y. Suzuki, D. Lew, A. F. Marshall, M. R. Beasley, and T. H. Geballe, Phys. Rev. B **48**, 10642 (1993).

[17] G. G. Li, F. Bridges, J. B. Boyce, and W. C. H. Joiner, Phys. Rev. B **47**, 12110 (1993).

[18] T. Ito, K. Takenaka, and S. Uchida, Phys. Rev. Lett. **70**, 3995 (1993); A. Carrington, A. P. Mackenzie, C. T. Lin, and J. R. Cooper, Phys. Rev. Lett. **69**, 2855 (1992).

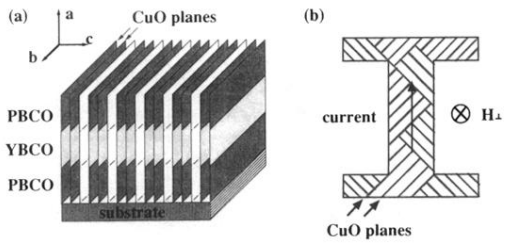

FIG. 1. (a) A schematic of a grain of an *a* axis YBCO/PBCO superlattice. (b) Current and field configurations of the superlattices.